Search for the radion using the ATLAS detector

G. Azuelos, D. Cavalli, H. Przysiezniak, L. Vacavant

▶ To cite this version:

HAL Id: in2p3-00014135
http://hal.in2p3.fr/in2p3-00014135

Submitted on 18 Nov 2003

Search for the Radion using the ATLAS Detector

G. Azuelos[1], D. Cavalli[2], H. Przysiezniak[3] and L. Vacavant[4]

[1] Laboratoire RJA Lévesque, Université de Montréal, Montréal, Québec, H3C 3J7, CANADA
[2] Dipartimento di Fisica, Università di Milano e INFN Sezione di Milano, I-20133 Milano, ITALY
[3] Laboratoire de Physique des Particules, IN2P3-CNRS, F-74019 Annecy-le-Vieux, FRANCE
[4] Lawrence Berkeley National Laboratory, Physics Division, Berkeley CA 94720-8167, USA

Abstract. The possibility of observing the radion using the ATLAS detector at the LHC is investigated. Studies on searches for the Standard Model Higgs with the ATLAS detector are re-interpreted to obtain limits on radion decay to $\gamma\gamma$ and $ZZ^{(*)}$. The observability of radion decays into Higgs pairs, which subsequently decay into $\gamma\gamma + b\bar{b}$ or $\tau\tau + b\bar{b}$ is then estimated.

PACS. XX.XX.XX No PACS code given

1 Introduction

The hierarchy between the electroweak and Planck scales is one of the principal puzzles in models of unification of the interactions. The postulate of the existence of compactified large extra dimensions allows for a Planck scale in the TeV range, but transfers the problem to the unnatural size of the extra dimension(s). In the model of Randall and Sundrum (RS) [1], two 4-d surfaces (*branes*) bound a slice of 5-d space-time. The SM fields are assumed to be located on one of the branes (the TeV brane), while gravity lies in the bulk. The fifth dimension is not large, but the metric is non-factorizable, allowing for a resolution of the hierarchy problem, given an appropriate warp factor. The theory admits two types of four-dimensional massless excitations: the usual graviton and a graviscalar, the modulus or radion (ϕ). In order to stabilize the size of the extra dimension without fine tuning of parameters, Goldberger and Wise [2] have proposed a mechanism by which the radion acquires a mass, expected to be smaller than the J=2 Kaluza-Klein excitations. The presence of the radion is one of the important phenomenological consequences of these theories of warped extra dimensions [3–12]. The study of this scalar therefore constitutes a crucial probe of the model.

1.1 Radion branching ratios and width

The radion couplings to fermions and bosons are similar to those of the Standard Model (SM) Higgs [3]; only their relative strengths change. They are expressed as a function of three parameters: the physical mass of the radion m_ϕ, the vacuum expectation value of the radion or scale, Λ_ϕ, and the radion-SM Higgs mixing parameter ξ [3,13,14].

In the following study, it is assumed that the SM Higgs has been discovered and that its mass has been measured. The branching ratios of the radion are calculated using those of the SM Higgs as calculated in HDECAY [15], and using the ratio of the radion to Higgs branching ratios given by [3]. For the mixing scenarios considered here, ($\xi = 0$ and $\xi = 1/6$), the branching ratios of the light Higgs are essentially SM-like [14].

Figure 1 shows the principal branching ratios as a function of scalar mass for decays of the SM Higgs (top plots) and of the radion when $m_h = 125$ GeV and $\Lambda_\phi = 1$ TeV, for $\xi = 0$ when there is no ϕ-h mixing (middle plots), and for $\xi = 1/6$ when ϕ and h are heavily mixed (bottom plots). These figures present the following features:

- $BR(\phi \to gg)$ is greatly enhanced with respect to the Higgs and is close to unity for $m_\phi > 500$ GeV and $\xi = 1/6$,
- the radion decays into two SM Higgs for $m_\phi \geq 2m_h$,
- $BR(\phi \to \gamma\gamma)$ is enhanced for $\xi = 1/6$ and $m_\phi \sim 600$ GeV,
- for $\xi = 1/6$ an interference is observed, producing a strong suppression of decays to vector bosons at a particular mass of the radion.

The radion has a very narrow natural width. Figure 2 shows the total width as a function of mass, for the SM Higgs and for the radion with $\xi = 0$ and $1/6$, for $\Lambda_\phi = 1$ TeV. The width is inversely proportional to the square of Λ_ϕ.

The aim of the present study is to investigate the possibility of observing a RS radion with the ATLAS detector through the following decays: $\phi \to \gamma\gamma$, $\phi \to ZZ^{(*)} \to 4\ell$, $\phi \to hh \to b\bar{b}\gamma\gamma$ and $\phi \to hh \to b\bar{b}\tau^+\tau^-$. Only the direct production of the radion $gg \to \phi$ is considered since
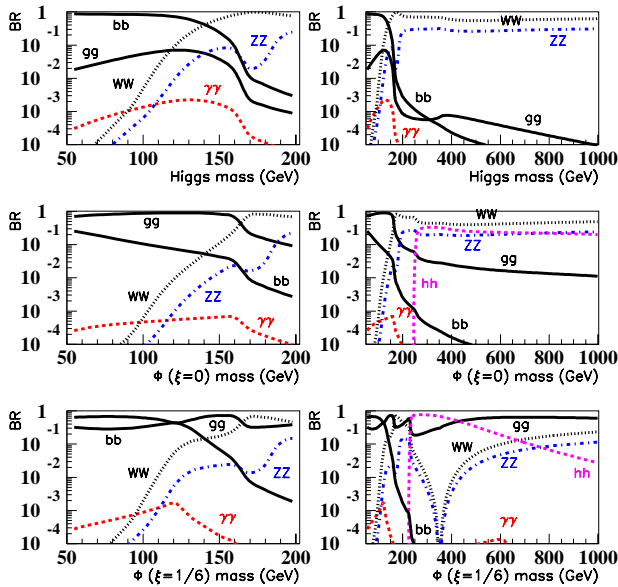
Fig. 1. Branching ratios of the SM Higgs (top), and of the radion when $\xi = 0$ (middle) and $\xi = 1/6$ (bottom) as a function of their mass, for $\Lambda_\phi = 1$ TeV. The Higgs mass in the four lower plots is set to $m_h = 125$ GeV.
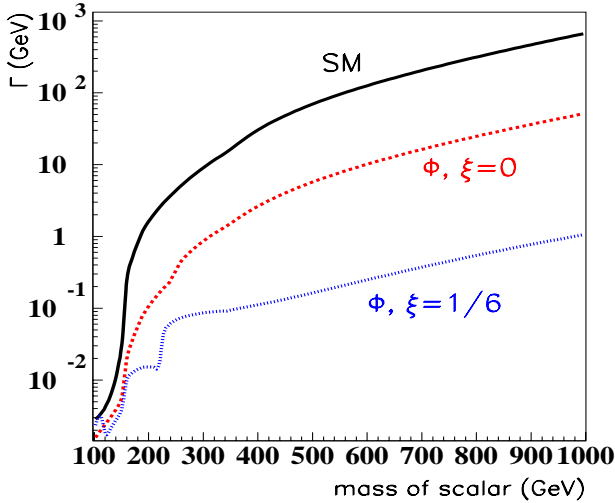

Fig. 2. Width of the SM Higgs and of the radion with $\xi = 0$ and $1/6$ both for $\Lambda_\phi = 1$ TeV.

it is the main process at LHC and it benefits from the enhancement of the coupling ϕgg.

Other signals, observable in SM Higgs decay [16], such as $H \to WW \to \ell\nu\ell\nu$, should be observable in the corresponding radion decay channel [11]. The mass reconstruction is difficult in this case, but observation of the signal would help confirm the discovery.

2 $\phi \to \gamma\gamma$ and $\phi \to ZZ^{(*)} \to 4\ell$

For the $\gamma\gamma$ ($m_\phi < 160$ GeV) and $ZZ^{(*)}$ ($m_\phi > 100$ GeV) decay channels, the radion signal significance is determined from the SM Higgs results expected for ATLAS [16], for 100 fb^{-1} (one year at high luminosity 10^{34} cm^{-2}s^{-1}). Evaluating the signal significance as $S/\sqrt{B}$, where S and B are the numbers of signal and background events respectively, the ratio of the radion signal significance over that of the SM Higgs, is given by [3]:

$$\frac{S/\sqrt{B}(\phi;\gamma\gamma,ZZ)}{S/\sqrt{B}(h;\gamma\gamma,ZZ)} = \frac{\Gamma_{\phi\to gg}BR(\phi\to\gamma\gamma,ZZ)}{\Gamma_{h\to gg}BR(h\to\gamma\gamma,ZZ)}\sqrt{\frac{\sigma_h^{\gamma\gamma,ZZ}}{\sigma_\phi^{\gamma\gamma,ZZ}}}$$

Accounting for experimental resolution, the ZZ resonance width is given by $\sigma_{h,\phi}^{ZZ} = \sqrt{(\Gamma_{tot}^{h,\phi}/2.36)^2 + (0.02 m_{h,\phi})^2}$, where $\Gamma_{tot}^{h,\phi}$ is the total intrinsic width of the Higgs or ϕ resonance. In the energy range considered, the $\gamma\gamma$ resonance width is essentially independent of the negligible intrinsic width of the resonance, $\sigma_{h,\phi}^{\gamma\gamma} = 0.10\sqrt{m_{h,\phi}} + 0.005 m_{h,\phi}$, and in this case, the last factor is simply unity. Using the ATLAS SM Higgs signal significance results [16], the radion signal significance is determined and shown in Figure 3 as a function of the mass of the radion, for the $\gamma\gamma$ channel (top) and for the $ZZ^{(*)}$ channel (bottom), for $\Lambda_\phi = 1,10$ TeV, $\xi = 0,1/6$, and for an integrated luminosity of 100 fb^{-1}.
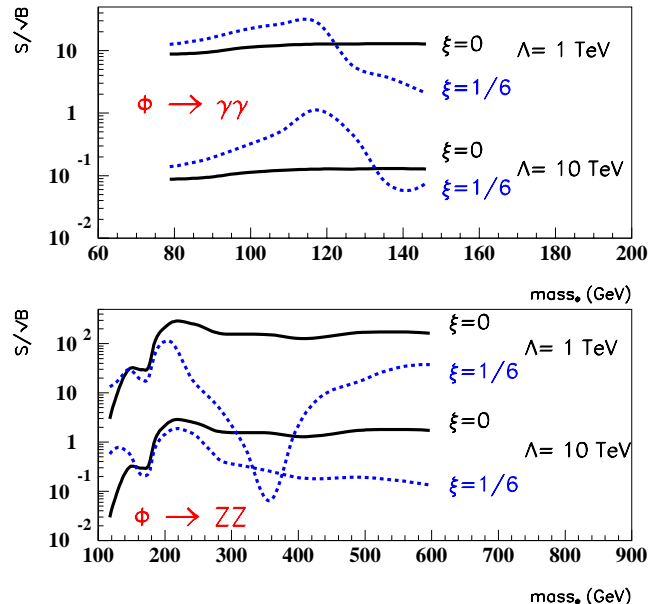

Fig. 3. Signal significance versus the mass of the radion, for the $\gamma\gamma$ channel (top) and for the $ZZ^{(*)}$ channel (bottom). In both plots, the values for $\Lambda_\phi = 1,10$ TeV and $\xi = 0,1/6$ are shown, for an integrated luminosity of 100 fb^{-1}.

3 Radion production at the LHC

From the SM Higgs production cross section, evaluated at next to leading order in [17], the cross section for radion production was estimated according to:

$$\sigma(gg \to \phi) = \sigma(gg \to h) \cdot \frac{\Gamma(\phi)}{\Gamma(h)} \frac{BR(\phi \to gg)}{BR(h \to gg)}$$

where Γ is the total width of the radion or Higgs resonance, shown in Fig. 2 and the branching ratios to a pair of gluons are shown if Fig. 1.

In the following sections, for the purpose of estimating the limits of observation of radion decay to a pair of SM Higgs bosons, two reference values are taken for the mass of the radion: 300 GeV and 600 GeV. The production cross sections in these cases are 58 pb and 8 pb respectively.

4 $\phi \to hh \to \gamma\gamma b\bar{b}$

As was mentioned in Section 1, the radion, similarly to the heavy Higgs of the Minimal SuperSymmetric Model (MSSM), can decay into Higgs pairs with relatively high branching ratio (see Figure 1). The specific decay channel $\phi \to hh \to \gamma\gamma b\bar{b}$ offers an interesting signature, with two high-p_T isolated photons and two b-jets. The background rate is expected to be very low for the relevant mass region $m_h > 115$ GeV and $m_\phi > 2m_h$. In addition, triggering on such events is easy and the diphoton mass provides very good kinematical constraints for the reconstruction of m_ϕ.

The decay $hh \to \gamma\gamma b\bar{b}$ was previously studied in the context of the MSSM Higgs [18], although the mass ranges investigated were lower. The approach and the selection used in this study are very similar.

4.1 Signal

Signal events were generated with PYTHIA 6.158 [19]. The heavy Higgs H^0 production process via gluon-gluon fusion (in the framework of the Minimal 1-Higgs doublet Standard Model) was used to produce the radion. The mass and the width of the H^0 were changed to reflect those of the radion while the light Higgs mass was set to $m_h = 125$ GeV.

As shown in Figure 2, the total width of the radion is a factor of 10 (100) smaller for $\xi = 0$ (1/6) than that of the Higgs, such that it is completely negligible with respect to the reconstructed mass resolutions.

Two samples of 100k events each were generated, for $m_\phi = 300$ GeV and for $m_\phi = 600$ GeV.

4.2 Background

The backgrounds for this channel are $\gamma\gamma b\bar{b}$ (irreducible), $\gamma\gamma c\bar{c}, \gamma\gamma bj, \gamma\gamma cj$ and $\gamma\gamma jj$ (reducible with b-tagging). The events were generated with PYTHIA 6.158. In the region of mass considered for the Higgs, the main production processes are the Born diagram $qq \to \gamma\gamma$ and the box diagram $gg \to \gamma\gamma$. The rates are therefore very low. However large uncertainties apply to these backgrounds since the jets arise only from initial state radiation and not from the hard-scattering. Generating a background sample of a sensible size turns out to be very CPU time consuming, and some cuts had to be applied at the event generation: the sample was generated in seven different bins of $\hat{p}_\perp$, the transverse momentum defined in the rest frame of the hard interaction. For each bin, ten million events were generated.

Single photon production in the hard process γj, accompanied by QCD or QED radiation, and where either the photon or jet is misidentified represents another reducible background. This process was studied in the context of the SM $H \to \gamma\gamma$ channel, and was found to increase the total background by a factor of two. In the context of the radion where the backgrounds are negligible, this is therefore not expected to affect the final results.

4.3 Detector simulation

The detector effects on the signal and background events are simulated with a fast Monte-Carlo code, ATLFAST 2.53 [20], based on parametrized detector response. While most parameters are chosen from the standard ATLFAST low luminosity conditions (10^{33} cm^{-2}s^{-1}), a few improvements were applied for this study:

- jets were recalibrated using a detailed parameterization,
- the photon reconstruction efficiency was assumed to be 80%,
- a p_T-dependent b-tagging parameterization was used with an average efficiency of $\epsilon_b = 60\%$ and rejection factors of approximately 93 for light-quark jets and 7 for c-jets, respectively [16].

4.4 Selection

To extract the signal, two isolated photons with $p_T > 20$ GeV and $|\eta| < 2.5$, and two jets with $p_T > 15$ GeV, $|\eta| < 2.5$ were required. At least one of the jets had to be tagged as a b-jet. The diphoton and the dijet invariant masses were then formed. Figure 4 shows the reconstructed invariant masses for $m_\phi = 300$ GeV, $\xi = 0$ and $\Lambda_\phi = 1$ TeV. Two mass window cuts were applied: $m_{\gamma\gamma} = m_h \pm 2$ GeV and $m_{bj} = m_h \pm 20$ GeV.

The photons and jets fulfilling these requirements were then combined to form the $m_{\gamma\gamma bj}$ invariant mass as shown in Figure 5. The mass resolution improves to 5 GeV when constraining the reconstructed masses m_{bj} and $m_{\gamma\gamma}$ to the light Higgs mass m_h, as shown on the right-hand plot of Figure 5. The signal acceptances after the various cuts described above are given in Table 1.

The same analysis procedure was applied to the background sample. Because of the uncertainties concerning the level of the background, as discussed in Section 4.2,
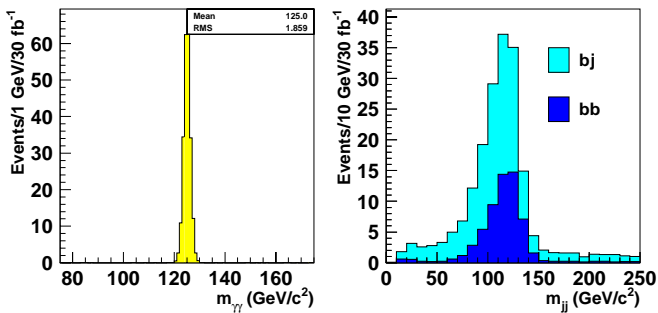
Fig. 4. Diphoton (left) and dijet (right) invariant mass distributions, for $m_\phi = 300$ GeV, $\xi = 0$, $\Lambda_\phi = 1$ TeV and 30 fb^{-1} (three years at low luminosity 10^{33} cm^{-2}s^{-1}). The right-hand plot shows the impact of requiring two b-tagged jets instead of one.
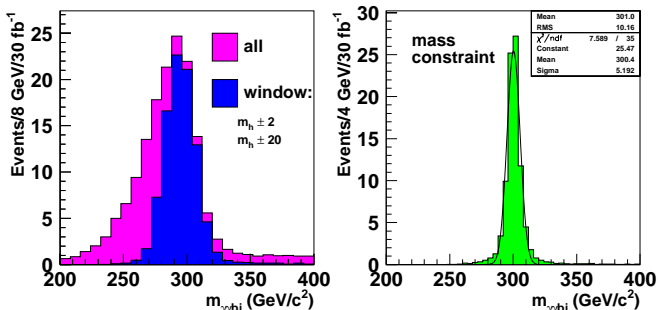

Fig. 5. Reconstructed $\gamma\gamma bj$ invariant mass distribution, for $m_\phi = 300$ GeV, $\xi = 0$, $\Lambda_\phi = 1$ TeV and for 30 fb^{-1}. The plots on the left show all combinations and the ones fulfilling the mass window cuts (cf. text). The distribution on the right is obtained by constraining the reconstructed masses m_{bj} and $m_{\gamma\gamma}$ to the light Higgs mass m_h, after the mass window cuts.

Cuts	$m_\phi = 300$ GeV	$m_\phi = 600$ GeV
photons kinematics	46%	51%
jets kinematics	36%	28%
b-tagging	76%	78%
$m_{\gamma\gamma}$ window cut	83%	85%
m_{bj} window cut	49%	53%
total	5%	5%

Table 1. Acceptance for the signal, for $\xi = 0$, $\Lambda_\phi = 1$ TeV and for the two radion masses studied. For each cut the acceptance is defined with respect to the previous one.

the mass window cuts were loosened to keep events fulfilling: $m_{\gamma\gamma} = m_h \pm 30$ GeV and $m_{bj} = m_h \pm 40$ GeV. The background level remains nevertheless extremely low, even in this conservative approach.

4.5 Results

The final candidate events are selected in a mass window $< m_{\gamma\gamma bj} > \pm 1.5\sigma_{m_{\gamma\gamma bj}}$ for signal and background. The results are given in Table 2.

	$m_\phi = 300$ GeV	$m_\phi = 600$ GeV
$\xi = 0, \Lambda_\phi = 1$ TeV	84.5	7.0
$\xi = 0, \Lambda_\phi = 10$ TeV	0.9	0.1
$\xi = 1/6, \Lambda_\phi = 1$ TeV	150.9	5.3
$\xi = 1/6, \Lambda_\phi = 10$ TeV	1.2	0.1
background	$1.42\ 10^{-4}$	0

Table 2. Number of events selected for signal and for background, for $m_\phi = 300$ and 600 GeV, for 30 fb^{-1} and for $m_h = 125$ GeV.

	$m_\phi = 300$ GeV	$m_\phi = 600$ GeV
$\xi = 0, \Lambda_\phi = 1$ TeV	4	(43)
$\xi = 0, \Lambda_\phi = 10$ TeV	(333)	N/A
$\xi = 1/6, \Lambda_\phi = 1$ TeV	2	(57)
$\xi = 1/6, \Lambda_\phi = 10$ TeV	(250)	N/A

Table 3. Minimum integrated luminosity (fb^{-1}) needed for discovery. N/A means that the signal is not accessible at LHC. Integrated luminosities larger than 30 fb^{-1} are in parentheses since the feasibility of the analysis at high luminosity has not been studied.

Since this channel is practically background free, a signal discovery is defined here as a minimum of ten events. The minimum integrated luminosities needed for discovery are listed in Table 3. A few fb^{-1} are needed for $\xi = 0$ if $\Lambda_\phi \sim 1$ TeV.

In the special case where $\xi = 0$, the cross-section is proportional to Λ_ϕ^{-2}. A lower limit on Λ_ϕ can therefore be derived from this study. It is obtained using the prescription of [21]: for a known mean background of zero, there is more than 95% chance of observing at least 10 events if the expected number of signal events is greater than 18. The corresponding reach in Λ_ϕ is 2.2 TeV for $m_\phi = 300$ GeV and 0.6 TeV for $m_\phi = 600$ GeV for an integrated luminosity of 30 fb^{-1}.

5 $\phi \to hh \to b\bar{b}\tau^+\tau^-$

The channel $\phi \to hh \to b\bar{b}\tau^+\tau^-$ provides another potentially interesting signal for radion discovery, although the background is higher and the reconstructed mass resolutions are poorer than in the $\phi \to hh \to \gamma\gamma b\bar{b}$ channel.

In order to provide a trigger, a leptonic decay of the τ is required. Here, only the case when one τ decays leptonically and the other hadronically is considered. As above, the events were generated by appropriately adapting the process of MSSM decay of the heavy Higgs H^0 into two light Higgs bosons (h) in Pythia 6.158 [19]. The effect of the ATLAS detector on the resolution and efficiency of reconstruction of these events was simulated with the ATLAS fast simulation package (ATLFAST 2.53). The efficiency for hadronic τ reconstruction was assumed to be

40%. The rejection against jets was calculated according to the parameterization obtained from fully simulated taus and jets in ATLAS [22].

For b-jet tagging, an efficiency of 60% was assumed, with rejection factors of 10 for c-jets and 100 for light jets, respectively [16].

5.1 Signal and background

As in the previous section, the radion mass values investigated are 300 and 600 GeV, while the Higgs mass is set to 125 GeV. The fast simulated samples are:

- $\phi \to hh \to b\bar{b}\ \tau^+\tau^-$. with one τ decaying leptonically and the other hadronically (10 000 events)
- $t\bar{t} \to bW^+\ \bar{b}W^-$ with one W decaying leptonically and the other hadronically (6×10^6 events).
- Z +jets, followed by $Z \to \tau^+\tau^-$ with one τ decaying leptonically and the other hadronically (4×10^6 events). Initial and final state radiation provide additional jets which can fake the signal. A cut of $\hat{p}_\perp > 15$ GeV was applied at generation level.
- W + jets, with the W bosons decaying leptonically (4×10^6 events). A cut of $\hat{p}_\perp > 15$ GeV was applied at generation level.

5.2 Selection

The study was performed assuming conditions of low luminosity (10^{33} cm^{-2}s^{-1}) since at high luminosity (10^{34} cm^{-2}s^{-1}) the $\tau\tau$ mass reconstruction efficiency is lower and the reconstructed $\tau\tau$ mass resolution is deteriorated by approximately a factor of two. Events were selected if they satisfied the following criteria:

- A lepton was present with $p_T^\ell > 25$ Gev, $|\eta^\ell| < 2.5$ (this lepton serves as a trigger).
- the transverse mass reconstructed from p_T^ℓ and $p_T^{\rm miss}$ was required to be < 40 GeV. This cut rejects background events containing W bosons.
- The $\tau\tau$ invariant mass was determined by combining the lepton with a tagged τ-jet having $p_T^{\rm jet} > 15$ GeV, $|\eta^{\rm jet}| < 2.5$ (see Figure 6). If more than one jet was tagged as a τ-jet, the combination with the mass nearest to m_h was chosen.
- A pair of b-tagged jets with $p_T > 15$ GeV and $|\eta| < 2.5$ was required (see Figure 6). If more than two jets were tagged as b-jets, the pair having the invariant mass closest to m_h was chosen.
- Cuts on the reconstructed $\tau\tau$ mass and $b\bar{b}$ mass were applied:
  $110 < m_{\tau\tau} < 140$ GeV and $90 < m_{b\bar{b}} < 140$ GeV in the case of the 300 GeV radion, and $110 < m_{\tau\tau} < 150$ GeV and $85 < m_{b\bar{b}} < 130$ GeV in the case of the 600 GeV radion.
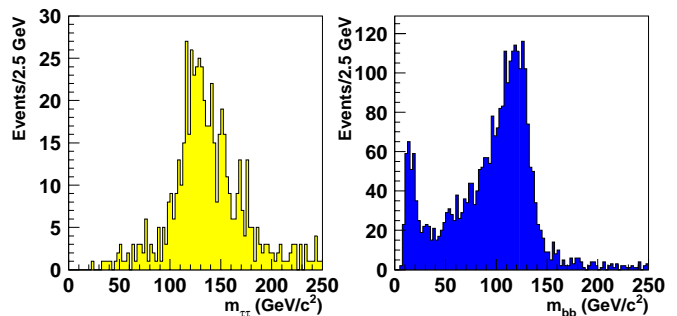

Fig. 6. Reconstructed $\tau\tau$ (left) and $b\bar{b}$ (right) invariant mass for the signal (arbitrary normalization).

Signal	$m_\phi = 300$ GeV	$m_\phi = 600$ GeV
$\sigma(gg \to \phi)$	58.0 pb	8.0 pb
$BR(\phi \to hh)$	0.33	0.23
$BR(hh \to \tau\tau bb)$	0.072	0.072
$BR(\tau\tau \to \ell + \text{hadrons})$	0.456	0.456
$\sigma \times BR =$	0.63 pb	0.062 pb
Background		
$t\bar{t} \to WbWb \to \ell + \text{hadrons}$		180 pb
$W + \text{jets}, W \to \ell\nu$		1.2×10^4pb
$Z + \text{jets}, Z \to \tau\tau \to \ell + \text{hadrons}$		350 pb

Table 4. Expected cross sections for $\Lambda_\phi =1$ TeV and $\xi = 0$ for signal and background before the event selection cuts ($\ell = e, \mu$).

5.3 Results

Although the signal efficiency is low, the background rejection is high. The expected cross sections for signal and background before the event selection are given in Table 4. The branching ratios account for leptonic decays into a muon or an electron.

Figure 7 shows the reconstructed masses for signal when m_ϕ=300 and 600 GeV respectively, for 30 fb^{-1}, $\Lambda_\phi = 1$ TeV and $\xi = 0$. The shape for a 300 GeV radion resonance is not distinguishable from the background (mostly $t\bar{t}$). Therefore systematic errors will most probably be dominated by the understanding of the level of this background.

The expected number of events for an integrated luminosity of 30 fb^{-1} are given in Table 5 for the two radion masses and for the backgrounds, when $\xi = 0$ and $\Lambda_\phi = 1$ TeV. The signal and background were evaluated in mass windows of 260-340 GeV and 540-660 GeV for radion masses of 300 GeV and 600 GeV respectively.

Requiring a minimum of 10 events and $S/\sqrt{B} \geq 5$, the maximum reach in Λ_ϕ is 1.04 TeV for both m_ϕ=300 GeV and m_ϕ=600 GeV, but the uncertainties in background subtraction may affect considerably the observability of this channel in the first case.
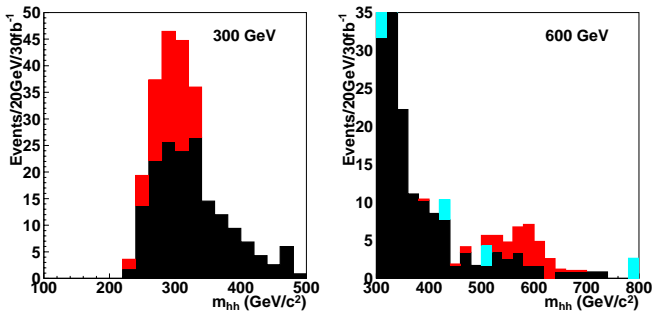
Fig. 7. Reconstructed mass of the radion, for 30 fb^{-1} and $\Lambda_\phi = 1$ TeV, $\xi = 0$. Left plot: expected signal (light) and $t\bar{t}$ background (dark). Right plot: $t\bar{t}$ background (dark), expected signal (light) and Z+jets background (very light).

	m_ϕ=300 GeV	m_ϕ=600 GeV
Signal	57	17.1
$t\bar{t}$	98	10
Z + jets	13	0
W + jets	0	0
$S/\sqrt{B}$	5.4	5.4

Table 5. Expected number of events for signal and background, for an integrated luminosity of 30 fb^{-1} for m_ϕ =300 and 600 GeV, $\xi = 0$ and $\Lambda_\phi = 1$ TeV, after all cuts.

6 Conclusion

We have studied the possibility of observing the radion using the ATLAS detector at the LHC. The radion has couplings similar to those of the SM Higgs, and mixes with it, but it also has a large effective coupling to gluons. Re-interpreting results of previous studies on the search for a SM Higgs in ATLAS, a significance for observing a radion decaying into $\gamma\gamma$ or $ZZ^{(*)}$ has been determined as a function of its mass (see Figure 3). For an integrated luminosity of 100 fb^{-1}, the values $S/\sqrt{B}$ ~10 (0.1) are obtained for the $\gamma\gamma$ channel, with a mixing parameter ξ=0 and a scale Λ_ϕ=1 (10) TeV, in the range 80 GeV < m_ϕ < 160 GeV. For the $ZZ^{(*)}$ channel, $S/\sqrt{B}$ ~100 (1) for 200 GeV < m_ϕ < 600 GeV for the same conditions. Because the couplings are similar to those of the SM Higgs, a good measurement of the production cross section and branching ratios will be necessary to discriminate between the two scalars.

The radion can also decay into a pair of Higgs scalars, if the masses permit. Two cases were examined: $\phi \to hh \to \gamma\gamma b\bar{b}$ and $\phi \to hh \to \tau\tau b\bar{b}$, for radion masses of 300 and 600 GeV, for $m_h = 125$ GeV and for an integrated luminosity of 30 fb^{-1}. Limits on the maximal reach in Λ_ϕ were obtained for these two channels. For the $\gamma\gamma b\bar{b}$ channel, the background is negligible and the reach in Λ_ϕ is 2.2 (0.6) TeV for $m_\phi = 300$ (600) GeV, when ξ=0. For the $\tau\tau b\bar{b}$ channel, the reach for Λ_ϕ is about 1 TeV for both m_ϕ=300 GeV and m_ϕ=600 GeV, when ξ=0, although in the first case, uncertainties in the background shape may result in large systematic error.

Acknowledgements

References

1. L. Randall and R. Sundrum, *Phys. Rev. Lett.* **83**, 3370 (1999).
2. W.D. Goldberger and M.B. Wise, *Phys. Rev. Lett.* **83**, 4922 (1999).
3. G.F. Giudice, R. Rattazzi and J.D. Wells, *Nucl. Phys.* **595**, 250 (2001).
4. S.B. Bae, P. Ko, H.S. Lee and J. Lee, *Phys.Lett.* **B487** 299 (2000)
5. H. Davoudiasl, J.L. Hewett and T.G. Rizzo, *Phys.Rev.Lett.* **84** 2080 (2000)
6. K. Cheung, *Phys.Rev.* **D63** 056007 (2001)
7. H. Davoudiasl, J.L. Hewett and T.G. Rizzo, *Phys.Rev.* **D63** 075004 (2001)
8. G.D. Kribs, contribution to Snowmass 2001 [hep-ph/0110242].
9. T. Han, G.D. Kribs and B. McElrath *Phys.Rev.* **D64** 076003 (2001)
10. S.C. Park, H.S. Song and J. Song *Phys.Rev.* **D63** 077701 (2001)
11. M. Chaichian, A. Datta, K. Huitu and Z.H. Yu *Phys.Lett.* **B524** 161 (2002)
12. D. Dominici, B. Grzadkowski, J.F. Gunion, M. Toharia [hep-ph/0206197]
13. J.L. Hewett and T.G. Rizzo, contribution to Snowmass 2001 [hep-ph/0112343].
14. J.L. Hewett and T.G. Rizzo [hep-ph/0202155].
15. A. Djouadi, J. Kalinowski and M. Spira, *Comput. Phys. Commun.* **108** 56 (1998)
16. ATLAS Collaboration, Detector and Physics Performance, CERN/LHCC 99-14
17. M. Spira, Fortschr. Phys. 46 (1998) 203, (CERN-TH-97-068, hep-ph/9705337)
18. E. Richter-Was *et al.*, ATLAS Internal Note ATL-PHYS-96-074 (1996)
19. T. Sjöstrand, P. Edén, C. Friberg, L. Lönnblad, G. Miu, S. Mrenna and E. Norrbin, Computer Physics Commun. 135 (2001) 238.
20. E. Richter-Was, D. Froidevaux and L. Poggioli, ATLAS Internal Note ATL-PHYS-98-131 (1998)
21. R.D. Cousins and G.J. Feldman, *Phys. Rev.* **D57** 3873 (1998)
22. D. Cavalli and S. Resconi, ATLAS Internal Note ATL-PHYS-98-118 (1998)